2008

On well-balanced schemes for non-equilibrium flow with stiff source terms

W. Wang

C.-W. Shu

Helen Yee

On well-balanced schemes for non-equilibrium flow with stiff source terms

By W. Wang, C.-W. Shu†, H. C. Yee‡ AND B. Sjögreen¶

1. Motivation and objectives

In the modeling of unsteady reactive problems, the interaction of turbulence with finite-rate chemistry introduces a wide range of space and time scales, leading to additional numerical difficulties. A main difficulty stems from the fact that most numerical algorithms used in reacting flows were originally designed to solve non-reacting fluids. As a result, spatial stiffness due to reacting source terms and turbulence/chemistry interaction are major stumbling blocks to numerical algorithm development. One of the important numerical issues is the proper numerical treatment of a system of highly coupled stiff non-linear source terms, which will result in possible spurious steady state numerical solutions (see Lafon & Yee 1996).

It was shown in LeVeque (1998) that a well-balanced scheme, which can preserve the steady state solution exactly, may solve this spurious numerical behavior. The goal of this work is to consider a simple 1-D model with one temperature and three species as studied by Gnoffo, Gupta & Shinn (1989) and to study the well-balanced property of various popular linear and non-linear numerical schemes in the literature. The different behaviors of those numerical schemes in preserving steady states and in resolving small perturbations of such states will be shown.

2. Numerical methods

Assuming no conduction or radiation, the considered non-equilibrium models are a system of hyperbolic conservation laws with source terms, denoted by

$$U_t + F(U)_x = S(U). \tag{2.1}$$

Here U, $F(U)$ and $S(U)$ are column vectors with $m = ns + 2$ components where ns is the number of species.

$$U = (\rho_1, \ldots, \rho_{ns}, \rho v, \rho e_0)^T, \tag{2.2}$$

$$F(U) = (\rho_1 v, \ldots, \rho_{ns} v, \rho v^2 + p, \rho v e_0 + v p)^T, \tag{2.3}$$

$$S(U) = (s^1, \ldots, s^{ns}, 0, 0)^T, \tag{2.4}$$

where ρ_s is the density of species s. The total density is defined as $\rho = \sum_{s=1}^{ns} \rho_s$ and the pressure p is given by

$$p = RT \sum_{s=1}^{ns} \frac{\rho_s}{M_s}, \tag{2.5}$$

† Division of Applied Mathematics, Brown University, Providence, RI 02912
‡ NASA Ames Research Center, Moffett Field, CA 94035
¶ Lawrence Livermore National Laboratory, Livermore, CA 94551

where M_s is the molar mass of species s. The temperature T can be found from the total energy

$$\rho e_0 = \sum_{s=1}^{ns} \rho_s e_{i,s}(T) + \sum_{s=1}^{ns} \rho_s h_s^0 + \frac{1}{2}\rho v^2, \tag{2.6}$$

where $e_{i,s} = n_s RT/2M_s$ is the internal energy with $n_s = 3$ and 5 for monoatomic species and diatomic species, respectively, and the enthalpies h_s^0 are constants.

Let the Jacobian matrix $A = \partial F/\partial U$ with $(a^1, \ldots, a^m)$ being the eigenvalues of A,

$$(a^1, \ldots, a^m) = (v, \ldots, v, v + a, v - a), \tag{2.7}$$

where a is the so-called "frozen speed of sound". Denote R as the matrix whose columns are eigenvectors of A. Let $a^l_{j+1/2}, R_{j+1/2}$ denote the quantities a^l and R evaluated at some symmetric average of U_j and U_{j+1}. Define

$$\alpha_{j+1/2} = R^{-1}_{j+1/2}(U_{j+1} - U_j) \tag{2.8}$$

as the difference of the characteristic variables in the locally x direction.

In this report, the considered schemes are the fifth-order finite difference WENO schemes (Jiang & Shu 1989), second-order Semi-implicit Predictor-Corrector TVD (P-C TVD) (Yee & Shinn 1989; LeVeque & Yee 1990), second-order symmetric (Yee 1987) and Harten and Yee (Yee & Harten 1987; Yee 1989) TVD scheme and second-order MUSCL scheme (Yee 1989). Except for the P-C TVD, a third-order Runge-Kutta method is used for time discretization. When the source term is stiff, we apply the pointwise implicit additive Runge-Kutta (ARK) method (Kennedy & Carpenter 2003) instead.

3. Well-balanced properties and linear schemes

A well-balanced scheme refers to a scheme that preserves exactly specific steady state solutions of the governing equations.

We will first consider the 1-D scalar balance law, i.e., the steady state solution u satisfying

$$f(u, x)_x = g(u, x). \tag{3.1}$$

We define a linear finite difference operator D to be one satisfying $D(af_1 + bf_2) = aD(f_1) + bD(f_2)$ for constants a, b and arbitrary grid functions f_1 and f_2. A scheme for Eq. (2.1) is said to be a linear scheme if all the spatial derivatives are approximated by linear finite difference operators.

Xing & Shu (2006) proved that under the following two assumptions regarding Eq. (2.1) and the steady state solution of Eq. (3.1), linear schemes with certain restrictions are well-balanced schemes. Furthermore, high-order non-linear WENO schemes can be adapted to become well-balanced schemes.

Assumption 1. *The considered steady state preserving solution u of Eq.* (3.1) *satisfies*

$$r(u, x) = \textit{constant}, \tag{3.2}$$

for a known function $r(u, x)$.

Assumption 2. *The source term g(u,x) can be decomposed as*

$$g(u, x) = \sum_i s_i(r(u, x))t_i'(x) \tag{3.3}$$

for a finite number of functions s_i and t_i.

A linear scheme applied to Eq. (3.1) would have a truncation error

$$D(f(u,x)) - \sum_i s_i(r(u,x))D_i(t_i(x)), \tag{3.4}$$

where D and D_i are linear finite-difference operators used to approximate the spatial derivatives. One restriction to the linear schemes is needed:

$$D_i = D \quad \text{for all } i \tag{3.5}$$

when applied to the steady state solution. For such linear schemes we have

PROPOSITION 1. *For the balance law Eq.* (2.1) *with source term Eq.* (3.3)*, linear schemes with restrictions Eq.* (3.5) *for the steady state solutions satisfying* (3.2) *are well-balanced schemes.*

Proof. For the steady state solutions satisfying Eq. (3.2), the truncation error for such linear schemes with Eq. (3.5) reduces to

$$\begin{aligned} &D(f(u,x)) - \sum_i s_i(r(u,x))D(t_i(x)) \\ &= D\left(f(u,x) - \sum_i s_i(r(u,x))t_i(x)\right), \end{aligned}$$

where the linearity of D and the fact that $r(u,x)$ is constant for the steady state solution u are used. Note that for such steady state solution u, $f(u,x) - \sum_i s_i(r(u,x))t_i(x)$ is a constant, because

$$\begin{aligned} &\frac{d}{dx}\left(f(u,x) - \sum_i s_i(r(u,x))t_i(x)\right) \\ &= f(u,x)_x - \sum_i s_i(r(u,x))t_i'(x) \\ &= f(u,x)_x - g(u,x) = 0. \end{aligned}$$

Thus, the truncation error is zero for any consistent finite-difference operator D. Therefore, linear schemes with Eq. (3.5) preserve these steady state solutions exactly. □

We now consider high-order non-linear finite-difference WENO schemes in which the non-linearity comes from the non-linear weights and the smooth indicators. We follow the procedures described in Xing & Shu (2005, 2006). We first consider the situation without flux splitting (e.g., the WENO-Roe scheme in Jiang & Shu 1996). The WENO approximation to f_x can be written as

$$f_x|_{x=x_j} \approx \sum_{k=-r}^{r} c_k d_{k+j} = D_f(f)_j,$$

where $r = 3$ for the fifth-order WENO approximation and the coefficients c_k depend non-linearly on the smoothness indicators involving the grid function $f_{j-r}, \ldots, f_{j+r}$. The key idea now is to use the finite difference operator D_f, and apply it to approximate $t_i'(x)$ in

the source terms, i.e.,

$$t_i'(x_j) \approx \sum_{k=-r}^{r} c_k t_i(x_{k+j}) = D_f(t_i(x))_j.$$

Clearly, the finite-difference operator D_f, obtained from the high-order WENO procedure is a high-order linear approximation to the first derivative for any grid function. Therefore, the proof for Proposition 1 will be satisfied and we conclude that the high-order finite difference WENO scheme as stated above, without the flux splitting, and with the special handling of the source terms described above, maintains exactly the steady state.

The framework described for the scalar case can be easily applied to systems. For a system with m equations, we would have m relationships in the form of Eq. (3.2):

$$r_l(U, x) = \text{constant}, \quad l = 1, \ldots, m. \tag{3.6}$$

In Assumption 2, s_i could be arbitrary functions of $r_l(U, x)$, and s_i and t_i can be different for different components of the source vector. The characteristic decomposition procedure does not alter the argument presented for the scalar case (Xing & Shu 2005).

In this work, we first considered a three-species case ($\rho_1 = O$, $\rho_2 = O_2$, $\rho_3 = N_2$) with the following special steady state preserving case

$$\begin{cases} (\rho_1)_t = 0 \\ (\rho_2)_t = 0 \\ (\rho_3)_t = 0 \\ v = 0 \\ p = \text{constant} \\ S(U) = 0 \end{cases}. \tag{3.7}$$

The source term $S(U)$ has the form

$$S(U) = (2M_1\omega, -M_2\omega, 0, 0, 0), \tag{3.8}$$

where ω is the reaction progress variable

$$\omega = (k_f(T)\frac{\rho_2}{M_2} - k_b(T)(\frac{\rho_1}{M_1})^2)(\frac{\rho_1}{M_1} + \frac{\rho_2}{M_2} + \frac{\rho_3}{M_3}). \tag{3.9}$$

The forward and backward reaction rates k_f and k_b are functions of temperature

$$k_f = CT^{-2}e^{-E/T}, \tag{3.10}$$

$$k_b = k_f/k_{eq}, \tag{3.11}$$

where

$$k_{eq} = \exp(b_1^r + b_2^r \log z + b_3^r z + b_4^r z^2 + b_5^r z^3), \quad z = 10000/T. \tag{3.12}$$

Thus

$$r = S(U) = \text{constant}. \tag{3.13}$$

Note that x and U_x do not appear explicitly in $S(U)$ which is much simpler because all the $t_i'(x) = 1$. Thus any finite-difference operators D_i mentioned in Eq. (3.4) are absent. Therefore, as described above, linear schemes and WENO-Roe schemes applied to the steady state solution Eq. (3.7) for the problem Eq. (2.1) are well-balanced and maintain the original high-order accuracy.

Next, we will investigate the well-balanced properties of various TVD schemes mentioned in Sec. 2. The semi-implicit Predictor-Corrector TVD scheme (Yee & Shinn 1989;

LeVeque & Yee 1990) for the Eq. (2.1) has the form

$$\left[1-\frac{1}{2}\Delta t S'(U_j^n)\right]\Delta U_j^{(1)} = -\frac{\Delta t}{\Delta x}\left(F_j^n - F_{j-1}^n\right) + \Delta t S_j^n \tag{3.14}$$

$$U_j^{(1)} = \Delta U_j^{(1)} + U_j^n \tag{3.15}$$

$$\left[1-\frac{1}{2}\Delta t S'(U_j^n)\right]\Delta U_j^{(2)} = -\frac{\Delta t}{\Delta x}\left(F_{j+1}^{(1)} - F_j^{(1)}\right) + \Delta t S_j^n \tag{3.16}$$

$$U_j^{(2)} = \Delta U_j^{(2)} + U_j^{(1)} \tag{3.17}$$

$$U_j^{n+1} = U_j^n + \frac{1}{2}\left(\Delta U_j^{(1)} + \Delta U_j^{(2)}\right) + \left[R_{j+1/2}^{(2)}\Phi_{j+1/2}^{(2)} - R_{j-1/2}^{(2)}\Phi_{j-1/2}^{(2)}\right]. \tag{3.18}$$

The third step Eq. (3.18) acts as a non-linear filter step (Yee & Sjögreen 2007). The elements of the vector $\Phi_{j+1/2}$, denoted by $\phi_{j+1/2}^l$ with $l = 1, \ldots m$ are

$$\phi_{j+1/2}^l = \frac{1}{2}\left[\psi(\nu_{j+1/2}^l) - (\nu_{j+1/2}^l)^2\right]\left(\alpha_{j+1/2}^l - \hat{Q}_{j+1/2}^l\right), \tag{3.19}$$

where

$$\nu_{j+1/2}^l = \frac{\Delta t}{\Delta x}a_{j+1/2}^l. \tag{3.20}$$

The function $\psi(z)$ is an entropy correction to $|z|$

$$\psi(z) = \begin{cases} |z| & |z| \geq \delta_1 \\ (z^2+\delta_1^2)/2\delta_1 & |z| < \delta_1 \end{cases}, \tag{3.21}$$

where δ_1 is the entropy fix parameter. See Yee *et al.* (1991) for a discussion. $\hat{Q}_{j+1/2}^l$ is an unbiased limiter function which can be

$$\hat{Q}_{j+1/2}^l = \text{minmod}(\alpha_{j-1/2}^l, \alpha_{j+1/2}^l) + \text{minmod}(\alpha_{j+1/2}^l, \alpha_{j+3/2}^l) - \alpha_{j+1/2}^l \tag{3.22}$$

with

$$\text{minmod}(a,b) = \text{sgn}(a)\cdot\max\{0, \min[|a|, b\,\text{sgn}(a)]\}. \tag{3.23}$$

In this study, only diffusive limiters are considered. If we consider a "smooth" limiter, we replace the minmod function minmod(a,b) by the following smooth function

$$g(a,b) = [a(b^2+\delta_2) + b(a^2+\delta_2)]/(a^2+b^2+2\delta_2), \tag{3.24}$$

where δ_2 is a small parameter between 10^{-7} to 10^{-5}. The predictor step Eq. (3.14) and the corrector step Eq. (3.16) are linear. However, the last filter step is not linear. We will explore this further in the next section.

The numerical flux $\hat{F}_{j+1/2}$ for the second-order symmetric TVD scheme (Yee 1987) is described as

$$\hat{F}_{j+1/2} = \frac{1}{2}(F_j + F_{j+1} + R_{j+1/2}\Phi_{j+1/2}), \tag{3.25}$$

where

$$\phi_{j+1/2}^l = -\psi(a_{j+1/2}^l)(\alpha_{j+1/2}^l - \hat{Q}_{j+1/2}^l). \tag{3.26}$$

Similar to P-C TVD, the non-linearity of the TVD scheme comes from the $\hat{Q}_{j+1/2}^l$ part of the numerical flux Eq. (3.26).

The second-order Harten-Yee scheme (Yee & Harten 1987; Yee 1989) has the same form as Eq. (3.25) with

$$\phi^l_{j+1/2} = \frac{1}{2}\psi(a^l_{j+1/2})(g^l_j + g^l_{j+1}) - \psi(a^l_{j+1/2} + \gamma^l_{j+1/2})\alpha^l_{j+1/2}, \tag{3.27}$$

where

$$\gamma^l_{j+1/2} = \frac{1}{2}\psi(a^l_{j+1/2}) \begin{cases} (g^l_{j+1} - g^l_j)/\alpha^l_{j+1/2} & \alpha^l_{j+1/2} \neq 0 \\ 0 & \alpha^l_{j+1/2} = 0 \end{cases}. \tag{3.28}$$

Examples of the limiter function g^l_j can be

$$g^l_j = \text{minmod}(\alpha^l_{j-1/2}, \alpha^l_{j+1/2}) \tag{3.29}$$

or the smooth Eq. (3.24).

Unlike P-C TVD and the TVD schemes, the second-order MUSCL scheme (Yee 1989) is fully non-linear. The numerical flux for a MUSCL approach is expressed as

$$\hat{F}_{j+1/2} = \frac{1}{2}(F(U^R_{j+1/2}) + F(U^L_{j+1/2}) - \hat{R}_{j+1/2}\hat{\Phi}_{j+1/2}) \tag{3.30}$$

with

$$U^R_{j+1/2} = U_{j+1} - \frac{1}{2}\Delta_{j+1} \tag{3.31}$$

and

$$U^L_{j+1/2} = U_j + \frac{1}{2}\Delta_j. \tag{3.32}$$

The limiters can be

$$\Delta_j = \text{minmod}(U_{j+1} - U_j, U_j - U_{j-1}) \tag{3.33}$$

or the smooth Eq. (3.24). We can see that $U^R_{j+1/2}$ and $U^L_{j+1/2}$ bring non-linearity into every term of the flux Eq. (3.30).

4. Numerical study

This section performs a numerical study on two test problems to numerically verify whether the considered schemes are well-balanced and to study the associated behavior of these schemes.

4.1. *Well-balanced property*

First we numerically verify whether the considered schemes are well-balanced for the special stationary case Eq. (3.7) with

$$\rho_O = 4 \times 10^{-5}(1 + 0.2\sin(5\pi x)), \qquad p = 10^5, \quad v = 0, \tag{4.1}$$

with ρ_{O_2} and ρ_{N_2} are obtained by the equilibrium state condition. This set of steady state solutions is of the form Eq. (3.7). We choose Eq. (4.1) as the initial condition, and the results are obtained by time-accurate time-marching to the steady state.

The error and accuracy are listed in Tables 1 and 2. We can see that WENO-Roe, P-C TVD and TVD schemes are well-balanced schemes because they show machine round-off errors. However, WENO-LF and MUSCL schemes are not well-balanced. We remark that the super convergence of the results for WENO-LF and MUSCL is due to the simple form of the steady state solutions.

Numerically we have shown that P-C TVD and TVD schemes are well-balanced for

N	error	error	order
	WENO-Roe	WENO-LF	
40	5.64E-19	2.35E-09	–
80	4.73E-19	2.28E-11	6.69
160	6.46E-19	2.61E-13	6.45
320	9.58E-19	2.03E-15	7.00

TABLE 1. L^1 errors for ρ_O by WENO5 with N uniform grid points at $t = 0.01$.

N	error	error	error	error	order
minmod limiter	P-C TVD	symmetric TVD	Harten-Yee TVD	MUSCL	
40	9.09E-19	2.71E-21	1.02E-21	4.09E-09	–
80	1.05E-18	1.19E-21	3.39E-22	4.23E-10	3.27
160	1.20E-18	1.19E-21	1.36E-21	2.65E-11	4.00
320	1.38E-18	8.05E-22	5.51E-22	1.58E-12	4.07
smooth limiter					
40	6.95E-19	4.74E-21	2.37E-21	4.16E-08	–
80	8.33E-19	4.07E-21	1.69E-22	1.81E-09	4.52
160	8.70E-19	1.20E-19	1.36E-20	3.39E-11	5.73
320	1.05E-18	4.19E-21	7.62E-22	2.02E-12	4.07

TABLE 2. L^1 errors for ρ_O by TVD schemes with minmod/smooth limiter with N uniform grid points at $t = 0.01$, $\delta_1 = 0$.

the steady state solution Eq. (3.7). Even though the non-linear term $R\Phi$ in the P-C TVD and TVD schemes is non-linear, we will explain why this part will not destroy the well-balanced property in these schemes. Since they have similar formulas, we will use the symmetric TVD scheme as the example.

We claim that the function $\Phi = 0$ for the steady state problem Eq. (3.7). This is due to the fact that v is equal to zero in the steady state solution. By recalling the eigenvalue a in Eq. (2.7), it is easy to see that only the last two entries a^{ns+1} and a^{ns+2} are non-zero. The function ψ is in Eq. (3.21). If we set $\delta_1 = 0$, then we have $\psi(a^l) = |a^l|$. Therefore $\phi^1 \dots \phi^{ns}$ are always zeros. Note that for any $\delta_1 > 0$, P-C TVD and TVD schemes are not well-balanced.

Next, let us consider the factor $\alpha^l_{j+1/2} - \hat{Q}^l_{j+1/2}$ in Eq. (3.19) or Eq. (3.26), where $\alpha^l_{j+1/2}$ is given in Eq. (2.8). The resulting equations are obtained directly from the system

$$\alpha^{ns+1} + \alpha^{ns+2} = \Delta p/a^2, \tag{4.2}$$

$$\alpha^{ns+1} - \alpha^{ns+2} = (v\Delta\rho - \Delta(\rho v))/a, \tag{4.3}$$

where α, v and the frozen speed of sound a are evaluated at the Roe average at $j+1/2$, and $\Delta p = p_{j+1} - p_j$, etc. Since the pressure p is constant and velocity v is zero in the steady state solution, α^{ns+1} and α^{ns+2} are exactly zeros. Hence, the non-linear term $R\Phi$ is zero and then the P-C TVD and TVD schemes become linear schemes in the steady state solution Eq. (3.7). By Proposition 1, they are well-balanced schemes.

4.2. *Small perturbation*

In this section, we will demonstrate the advantages of the well-balanced schemes through the problem of a small perturbation over a stationary state.

The same stationary state solution Eq. (4.1) is considered, but with a small perturbation ϵ to the density is added to ρ_O, i.e.,

$$\rho'_O = \rho_O + \epsilon.$$

The other quantities are kept the same. At $t = 0.5$, we plot the differences between the perturbed solutions and the steady state solutions. The reference results are computed by WENO-Roe with 600 points and are considered to be "exact".

We first compare the results between WENO-Roe and WENO-LF. We add a $\epsilon = 10^{-10} \times \sin(\pi x)$ to the density ρ_O. To improve the viewing, a factor of 10^{10} is added to all the figures. The solution is depicted in Fig. 1(a). The well-balanced property of WENO-Roe clearly demonstrated with only 100 points to resolve such small perturbation. Although the solution indicates two small bumps in the density plot, these bumps disappear when the mesh is refined to 200 points.

Unlike the well-behaved WENO-Roe, the results by WENO-LF, which is not a well-balanced scheme, behave in a very oscillatory fashion using 100 grid points (see Fig. 1(b)). This is due to the fact that the well-balanced schemes can resolve the steady state solution exactly, hence they are able to resolve a very small perturbation. However, a scheme that is not well-balanced can only resolve the solution when the mesh is refined enough such that the truncation error of the scheme is much smaller than the perturbation. For example, when the mesh is refined to 300 points for WENO-LF (see Fig. 1(b)), the oscillations disappear and the solution is resolved.

Next, the numerical results by P-C TVD, TVD and MUSCL schemes are discussed, respectively. The minmod limiter and the corresponding smooth limiter Eq. (3.24) are considered. As indicated in Sec. 4.1, P-C TVD and TVD schemes produce machine round-off errors in computing the steady state solution, and analysis also shows that they are well-balanced schemes. Comparing these two schemes with the MUSCL scheme, which is not well-balanced, for the perturbation case, they perform better than MUSCL. For example, the MUSCL scheme has stronger oscillations than the P-C TVD and TVD schemes for a mesh $N = 300$ (see Figs. 2, 3, 4 and 5).

Note that in Figs. 2(a), 3(a) and 4(a), results for P-C TVD and TVD schemes with minmod limiter show some oscillations, and these oscillations do not disappear in the mesh refinement until the mesh is extremely fine. This might be caused by the lack of smoothness of the minmod limiter, which is continuous but not differentiable. When the minmod limiter is replaced by a smooth limiter, the solutions become smooth.

5. Future plans

The current results serve as a preliminary study on well-balanced schemes for non-equilibrium flow with source terms. Similar numerical investigation on a more realistic problem, such as a small perturbation of temperature over an equilibrium state, is planned

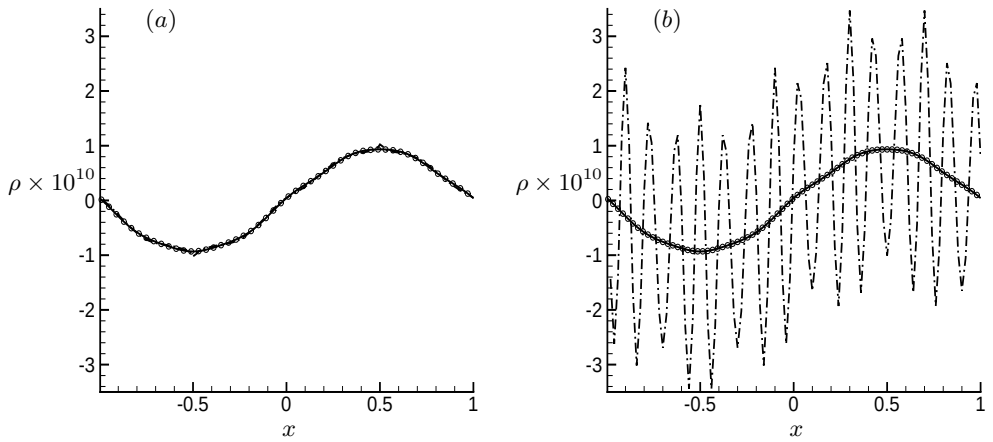

FIGURE 1. Results by WENO5: $\epsilon = 10^{-10} \times \sin(\pi x)$. (a) left: WENO-Roe (WENO-Roe 100: dash-dot; WENO-Roe 200: dotted with symbols; WENO-Roe 600: solid); (b) right: WENO-LF (WENO-LF 100: dash-dot; WENO-LF 300: dotted with symbols; WENO-Roe 600: solid).

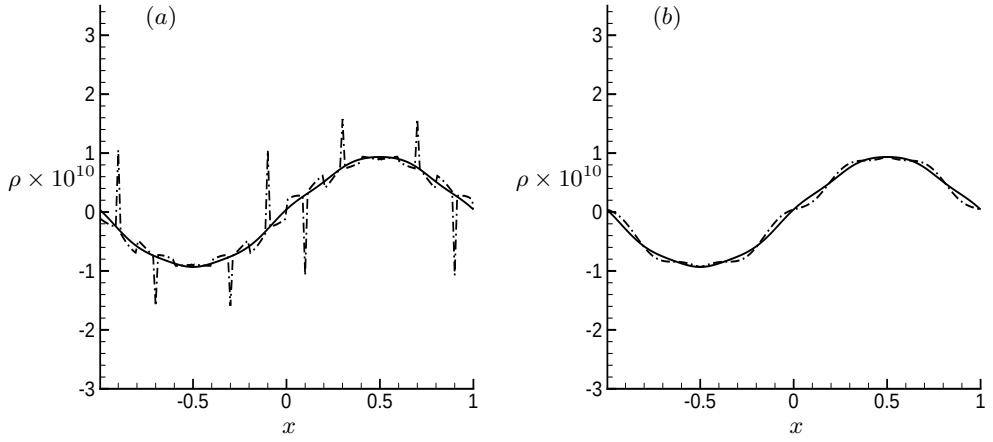

FIGURE 2. Results by semi-implicit Predictor-Corrector TVD : $\epsilon = 10^{-10} \times \sin(\pi x)$, $\delta_1 = 0$. (a) left: with minmod limiter; (b) right: with smooth limiter (P-C TVD 300: dash-dot; WENO-Roe 600: solid).

in the future. The same approach will be applied to analyze the well-balanced properties for the model with larger number of species and a more general type of steady state problem with non-zero velocity. In this case, the source terms are balanced by the flux gradients. Special attention will be paid to general reactive flows for which perturbation from equilibrium states could be small in some parts of the domain and large in other parts.

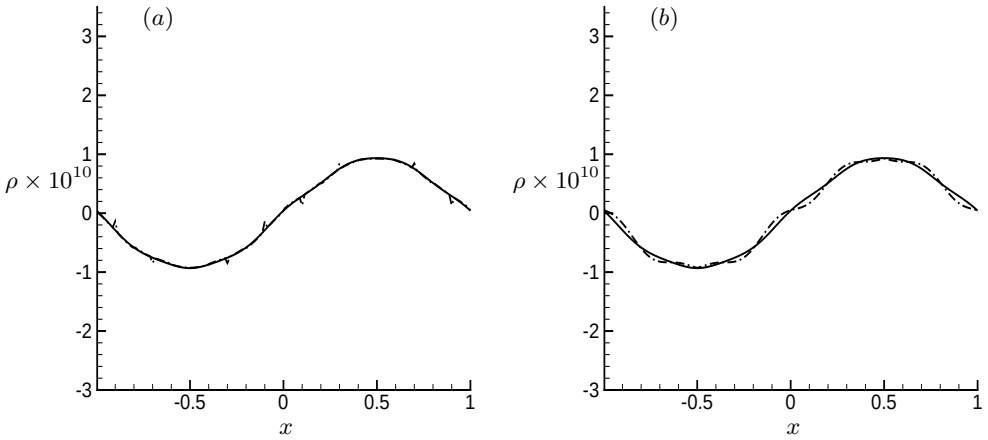

FIGURE 3. Results by symmetric TVD: $\epsilon = 10^{-10} \times \sin(\pi x)$, $\delta_1 = 0$. (a) left: with minmod limiter; (b) right: with smooth limiter (symmetric TVD 300: dash-dot; WENO-Roe 600: solid).

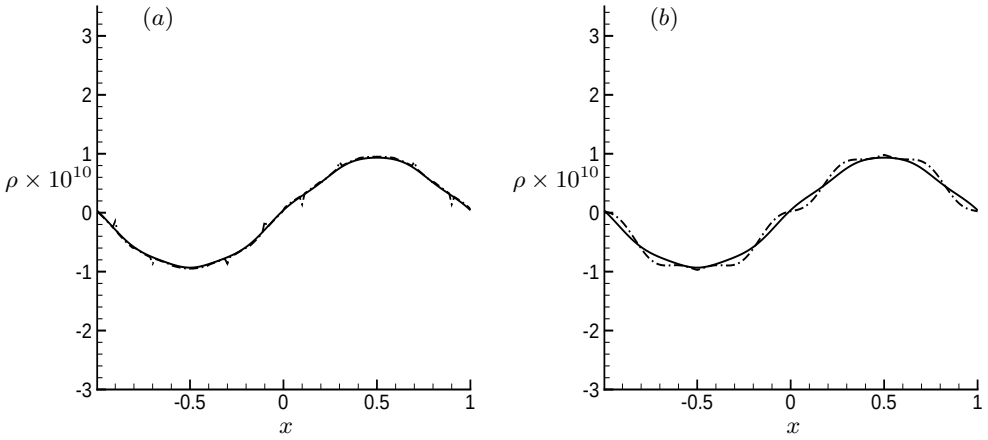

FIGURE 4. Results by Harten-Yee TVD: $\epsilon = 10^{-10} \times \sin(\pi x)$, $\delta_1 = 0$. (a) left: with minmod limiter; (b) right: with smooth limiter (Harten-Yee 300: dash-dot; WENO-Roe 600: solid).

Acknowledgments

The authors acknowledge the support of the DOE/SciDAC grant. The work by Bjorn Sjögreen performed under the auspices of the U.S. Department of Energy by Lawrence Livermore National Laboratory under Contract DE-AC52-07NA27344.

REFERENCES

GNOFFO, P. A., GUPTA, R. N. & SHINN, J. L. 1989 Conservation equations and physical models for hypersonic air flows in thermal and chemical nonequilibrium. *NASA Technical Paper* **2867**, 1–58.

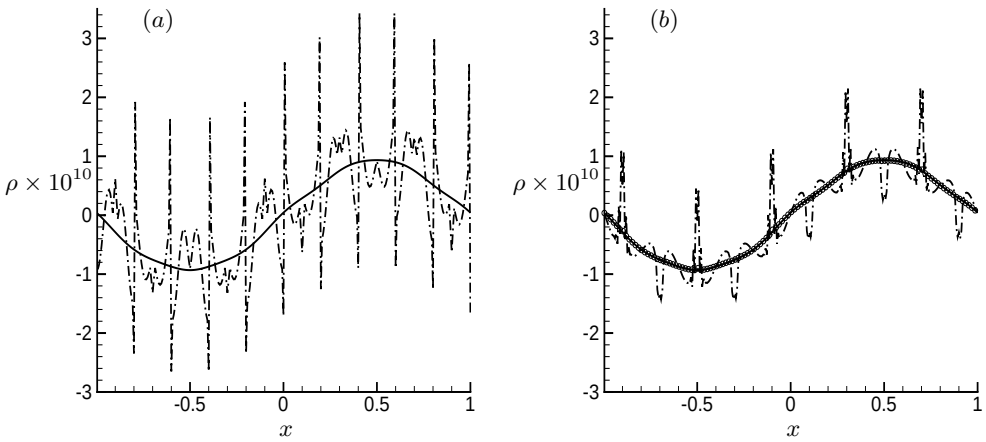

FIGURE 5. Results by MUSCL scheme: $\epsilon = 10^{-10} \times \sin(\pi x)$, $\delta_1 = 0$. (a) left: with minmod limiter; (b) right: with smooth limiter (MUSCL 300: dash-dot; WENO-Roe 600: solid).

JIANG, G. & SHU, C.-W. 1996 Efficient implementation of weighted ENO schemes. *J. of Comp. Phys.* **126**, 202–228.

KENNEDY, C. A. & CARPENTER, M. H. 2003 Additive Runge-Kutta schemes for convection-diffusion-reaction equations. *Appl. Numer. Math.* **44**, 139–181.

LAFON, A. & YEE, H. C. 1996 Dynamical approach study of spurious steady-state numerical solutions for non-linear differential equations, Part III: The effects of non-linear source terms in reaction-convection equations. *Comp. Fluid Dyn.* **6**, 1–36.

LAFON, A. & YEE, H. C. 1996 Dynamical approach study of spurious steady-state numerical solutions for non-linear differential equations, Part IV: Stability vs. numerical treatment of non-linear source terms. *Comp. Fluid Dyn.* **6**, 89–123.

LEVEQUE, R. J. 1998 Balancing source terms and flux gradients in high-resolution Godunov methods: the quasi-steady wave-propagation algorithm. *J. of Comp. Phys.* **146**, 346–365.

LEVEQUE, R. J. & YEE, H. C. 1990 A study of numerical methods for hyperbolic conservation laws with stiff source terms. *J. of Comp. Phys.* **86**, 187–210.

XING, Y. & SHU, C.-W. 2005 High order finite difference WENO schemes with the exact conservation property for the shallow water equations. *J. of Comp. Phys.* **208**, 206–227.

XING, Y. & SHU, C.-W. 2006 High order well-balanced finite difference WENO schemes for a class of hyperbolic systems with source terms. *J. of Sci. Comp.* **27**, 477–494.

YEE, H. C. 1987 Construction of explicit and implicit symmetric TVD schemes and their applications. *J. of Comp. Phys.* **68**, 151–179.

YEE, H. C. 1989 A class of high-resolution explicit and implicit shock-capturing methods. *VKI lecture series 1989-04, March 6-10, 1989; NASA TM-101088, Feb. 1989.*

YEE, H. C. & HARTEN, A. 1987 Implicit TVD schemes for hyperbolic conservation laws in curvilinear coordinates. *AIAA Journal* **25**, 266–274.

YEE, H. C. & SHINN, J. L. 1989 Semi-implicit and fully implicit shock-capturing methods for nonequilibrium flows. *AIAA Journal* **225**, 910–934.

Yee, H. C. & Sjögreen, B. 2007 Development of low dissipative high order filter schemes for multiscale Navier-Stokes/MHD systems. *J. of Comp. Phys.* **68**, 151–179.

Yee, H. C. , Sweby, P. K. & Griffiths, D. F. 1991 Dynamical approach study of spurious steady-state numerical solutions for non-linear differential equations, Part I: The dynamics of time discretizations and its implications for algorithm development in computational fluid dynamics. *J. of Comp. Phys.* **97**, 249–310.